3rd Specialty Conference on Material Engineering & Applied Mechanics
3e Conférence spécialisée sur le génie des matériaux et mécanique appliquée

Montréal, Québec
May 29 to June 1, 2013 / *29 mai au 1 juin 2013*

Performance of Concrete-Filled Light Gauge Steel Composite Columns: Pilot Study

W. L. Cortés-Puentes[1], A. Abdulridha[1], M. Majeed[1], D. Palermo[1], and B. Normand[2]
1 Faculty of Engineering, University of Ottawa, Ottawa, Ontario
2 B.J. Normand Ltd., Ottawa, Ontario

Abstract: A large-scale experimental program has recently been conducted on twelve concrete-filled light gauge steel composite columns, with the objective to quantify the axial load strength capacity. Currently, there is a lack of guidance for such structural elements. This system of construction (Mur-Tec Systems) is a novel forming system where structural beams and columns are placed in the cavities of prefabricated light gauge steel modular stud walls. The parameters investigated include column cross section size, length and cross section profile designated as A and B. The parameters investigated were representative of one-storey, full-scale construction. All columns were subjected to concentric axial loading in the horizontal position using two or three 1400-kN servo-hydraulic actuators. The test results illustrated that load capacity of the composite columns was proportional to the cross section. In addition, the measured compression shortening of the columns was proportional to the column length. In general, the columns with cross section profile B sustained higher load and greater compression shortening than those with profile A. All columns failed due to end bearing failure, including crushing of the concrete and local side wall buckling of the light gauge steel. The axial compression strength capacity of the concrete-filled light gauge steel columns was satisfactorily predicted based on end bearing resistance as the limiting state according to Canadian Standards Association Standard A23.3-04 Design of Concrete Structures including the contribution of the light gauge steel. The calculated to measured axial strength capacity was 0.93.

1 Introduction

Currently, there is a lack of prescribed design guidance for structural engineers to design concrete-filled light gauge steel columns. Therefore, there is a need for experimental data that can be used to corroborate design assumptions. Twelve concrete-filled light gauge steel composite columns, which are part of Mur-Tec Systems (a prefabricated non-traditional forming system), were tested under concentric axial loading to determine the axial compression strength capacity (Figure 1). Three parameters were investigated in the testing program: column length (8 ft and 9 ft), column cross section size (6 in x 6 in, 6 in x 12 in, and 6 in x 18 in), and cross section profile (A and B) of the light gauge steel. These parameters represent the full-scale arrangement of the columns as constructed in the field. The columns were instrumented and the response was continually monitored during testing. These included strain gauges on the light gauge steel encasing to record the axial straining, and displacement cable transducers to record the axial shortening of the columns under loading and to measure out-of-plane displacements of the column at mid-length. In addition to the experimental program, analytical calculations were conducted to predict the axial compression strength capacity of the concrete-filled light gauge steel columns. These calculations were based on the end bearing resistance as the limiting state according to the Canadian Standards Association (CSA) Standard A23.3-04 (2004), Design of Concrete Structures, including the contribution of the light gauge steel.

Figure 1: Mur-Tec Systems.

2 Experimental Program

2.1 Specimens

The experimental program consisted of compression tests of twelve light gauge steel composite columns with the geometric properties provided in Table 1. The columns were named according to the depth, the confinement profile, and the length of the column. In general, the specimens were named C$\#_1$-X$\#_2$. The letter C denotes "Column", the number $\#_1$ denotes the cross section depth in inches, the letter X denotes the light gauge steel profile, and the number $\#_2$ refers to the member length in feet. The light gauge steel had a gauge size of 18 (1.02 mm thickness) and the confinement profiles were denoted A and B. All columns had the same width of 6 in and three different depths: 6 in, 12 in, and 18 in. The columns were either 8 ft or 9 ft long.

Table 1: Column specimen properties.

Specimen	Light Gauge Steel Profile	Member Dimensions	
		Cross Section (in x in)	Length (ft)
C6-A8-1	A	6 x 6	8
C6-A8-2	A	6 x 6	8
C6-A9	A	6 x 6	9
C6-B9	B	6 x 6	9
C12-A8	A	6 x 12	8
C12-A9	A	6 x 12	9
C12-B8	B	6 x 12	8
C12-B9	B	6 x 12	9
C18-A8	A	6 x 18	8
C18-A9	A	6 x 18	9
C18-B8	B	6 x 18	8
C18-B9	B	6 x 18	9

Cross sectional details of the different components in the columns are shown in Figure 2. The columns were constructed from single 6 in x 6 in units. Therefore, the 6 in x 12 in and 6 in x 18 in columns were fabricated from 2 and 3 single units, respectively.

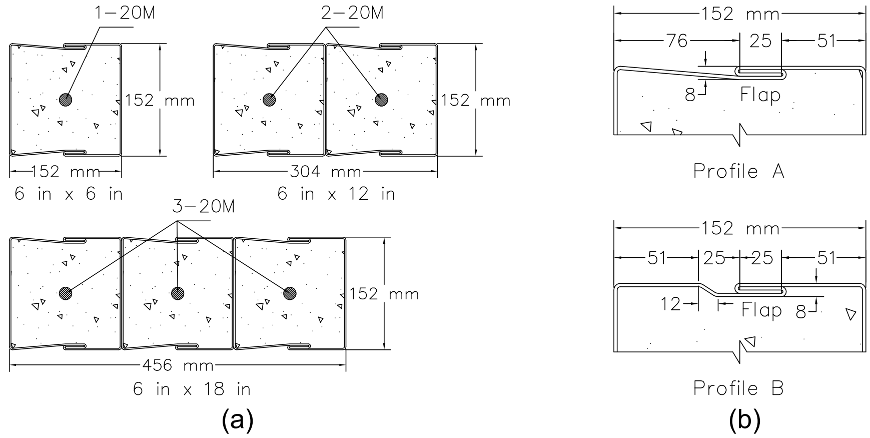

Figure 2: Column cross sections: (a) Typical cross sections (Profile A); and (b) Detail of profiles A and B.

2.2 Material Properties

Mechanical properties of the materials were established by conducting tensile testing of two coupons of the light gauge steel used to construct the columns in accordance with ASTM A370 (2009) and compression testing of three standard concrete cylinders (100 mm in diameter x 200 mm in height) in accordance with ASTM C39 (1994). The light gauge steel responded with a stress-strain curve characterized by three regions: an initial linear elastic part, a yielding plateau, and a strain hardening region (Figure 3(a)). Furthermore, there is a descending branch wherein the stress decreases until fracture occurs (Figure 3(a)). The recorded average properties of the light gauge steel were: yield strength, F_y, of 429 MPa, and corresponding yield strain, ε_y, of 0.24%; ultimate strength, F_u, of 531 MPa, and corresponding ultimate strain, ε_u, of 4.0%; rupture strain, ε_{rup}, of 6.5%; and modulus of elasticity, E_s, of 204000 MPa. The reinforced concrete responded with a non-linear behaviour with an initial elastic range up to approximately 80% of the peak strength followed by a parabolic response until failure (Figure 3(b)). An average compressive strength, f'_c, of 34 MPa, a corresponding strain, ε_c, of 0.23%, and modulus of elasticity, E_c, of 18550 MPa was recorded for the concrete cylinders.

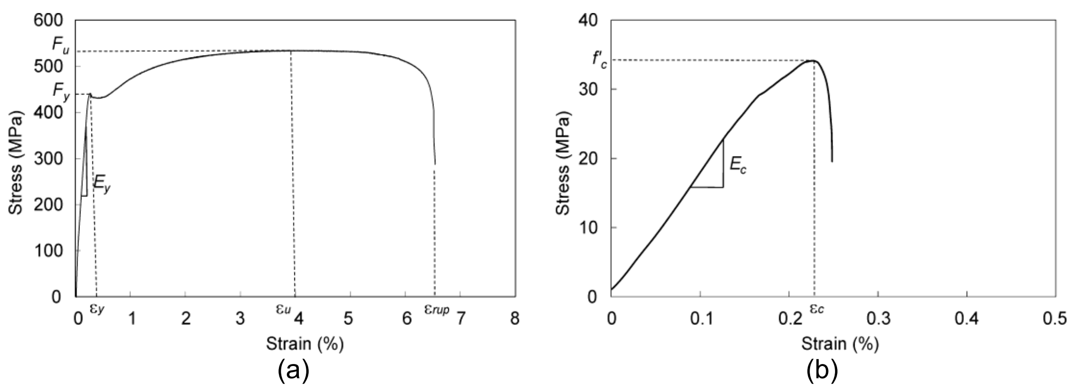

Figure 3: Stress-strain response of materials: (a) Light gauge steel; and (b) Concrete.

2.3 Test Setup

Forces imposed on the columns, axial and lateral displacements experienced by the columns, and longitudinal axial straining of the light gauge steel of each column were monitored and recorded during testing. The testing assembly consisted of an axial loading system in which the loading was applied in displacement-controlled mode using actuators positioned between reaction frames and a loading beam to simulate pin-pin support conditions. Two test assemblies were used depending on the capacity of the columns (Figure 4). Assembly one (Figure 4(a)) consisted of two actuators for testing columns C6 (6 in x 6 in) and columns C12 (6 in x 12 in). The columns were placed between the actuators and connected to the loading beam at one end and to a reaction frame at the other end. The two actuators pulled on the loading beam, which, in turn, imposed compressive forces on the columns. Assembly two (Figure 4(b)) consisted of three actuators for testing columns C18 (6 in x 18 in). The actuators were placed in parallel between the loading beam at one end and reaction frames at the other end. The columns were positioned on the opposite side of the loading beam and extended to a reaction frame. The three actuators pushed on the loading beam, which, in turn, imposed compression loading on the columns.

(a) (b) (c)

Figure 4: Test assembly: (a) Two actuators; (b) Three actuators; and (c) Instrumentation.

Each test specimen was instrumented with strain gauges and displacement measuring devices (Figure 4(c)). The longitudinal strains in the light gauge steel at the middle of the column were measured by electrical resistance strain gauges. Three strain gauges were bonded to the light gauge steel: one at the top and two on the sides of the column faces. On Columns C6, a fourth strain gauge was added at the bottom. The column displacements were measured using four Displacement Cable Transducers (DCTs). Two DCTs were placed at the mid-length of the columns to record out-of-plane displacements, and the other two DCTs were placed at the ends of the loading beam to monitor axial shortening of the columns and rotation of the loading beam.

3 Experimental Results

Results from the experimental program are presented in Tables 2 and 3, and Figure 5. Recorded peak loads and corresponding displacements are summarized in Table 2, axial load-shortening responses are shown in Figure 5, and maximum strains at peak load on the light gauge steel and lateral displacements recorded at the mid-length of the columns are reported in Table 3.

Table 2: Recorded peak forces and corresponding displacements for composite columns.

Specimen	Actuator 1		Actuator 2		Actuator 3 [a]	Total	
	Load (kN)	Displacement (mm)	Load (kN)	Displacement (mm)	Load (kN)	Load (kN)	Avg. Displacement (mm)
C6-A8-1	373	12.5	372	17.4	-	745	14.9
C6-A8-2	324	12.6	327	18.1	-	651	15.4
C6-A9	416	30.3	431	29.3	-	847	29.8
C6-B9	403	25.7	407	8.8	-	810	17.3
C12-A8	754	22.5	763	25.1	-	1517	23.8
C12-A9	694	33.6	706	15.2	-	1400	24.4
C12-B8	874	Not Recorded	879	23.7	-	1753	23.7
C12-B9	833	25.9	823	30.1	-	1656	28.0
C18-A8	846	23.0	761	25.6	801	2408	24.3
C18-A9	877	17.7	950	28.4	849	2676	23.1
C18-B8-1	908	20.2	919	24.6	-	1827	22.4
C18-B8-2	882	8.9	938	29.2	-	1820	19.1
C18-B9	833	27.6	897	33.1	765	2495	30.4

[a] Displacement of the loading beam at the location of Actuator 3 was not recorded.

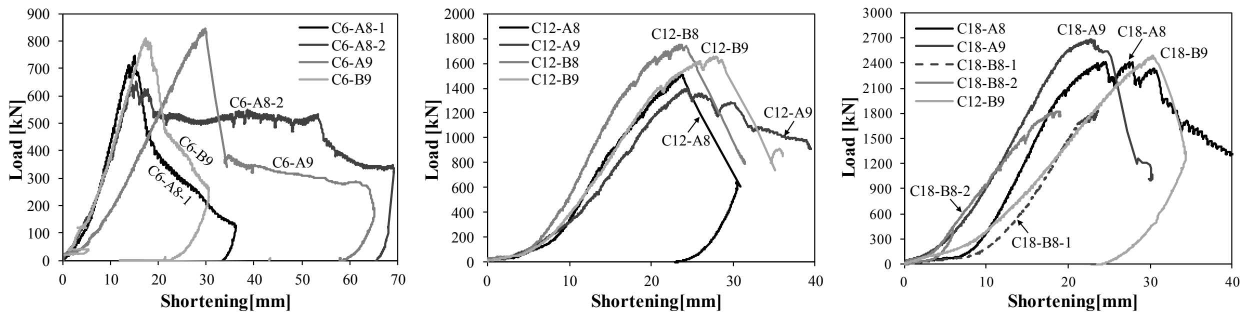

(a) (b) (c)

Figure 5: Recorded responses for columns: (a) Columns C6; (b) Columns C12; and (c) Columns C18.

Table 3: Strains and displacements recorded at mid-length of columns.

Specimen	Light Gauge Strain [a] (%)	Horizontal Displacement [b] (mm)	Vertical Displacement [b] (mm)
C6-A8-1	0.12	2.2	3.1
C6-A8-2	0.07	3.3	3.6
C6-A9	0.12	1.3	1.0
C6-B9	0.10	4.1	0.6
C12-A8	0.09	1.4	4.3
C12-A9	0.07	6.7	3.0
C12-B8	0.09	6.3	7.2
C12-B9	0.07	5.3	1.5
C18-A8	0.09	2.4	3.4
C18-A9	0.05	15.5	4.2
C18-B8-1	0.13	1.2	3.1
C18-B8-2	0.06	3.2	0.9
C18-B9	0.10	5.8	3.4

[a] Maximum strain at peak load recorded at the column faces

[b] Maximum displacement measured at mid-length of columns prior to peak load

3.1 Columns C6 (6 in x 6 in)

Loading of Columns C6 was conducted with two actuators. A small difference between the displacements of the two actuators was recorded through the test for Columns C6-A8-1, C6-A8-2 and C6-A9 as a result of a slight misalignment of the loading beam (Table 2). This difference, however, was significant for Column C6-B9 (Table 2). Despite the misalignment of the loading beam, the actuators applied equal forces that resulted in compression-only stresses in the column without inducing any moments. Shortening of Columns C6 was taken as the average of the displacements measured by the two cable transducers located at the loading beam. Damage of Columns C6 was observed as end bearing failure that involved compressive damage of the concrete, the confining light gauge steel and the internal steel (Figure 6). Failure initiated with bulging of the confining light gauge steel section at one end of the columns as a result of high compressive stresses. At higher loads, the light gauge steel buckled locally while the concrete near the buckled steel crushed. In some columns, the 20M internal reinforcing bar buckled due to the lack of lateral restraining, which was observed after removing the crushed concrete at the ends of the column.

(a) (b) (c) (d)

Figure 6: Damage of Columns C6 at failure: (a) C6-A8-1; (b) C6-A8-2; (c) C6-A9; and (d) C6-B9.

3.2 Columns C12 (6 in x 12 in)

Loading of Columns C12 was conducted with two actuators. A small difference in displacement between the two actuators was recorded through the test as a result of a slight misalignment of the loading beam for Columns C12-A8 and C12-B9 (Table 2), while the difference in displacements was higher for Column C12-A9 (Table 2). No induced moments resulted from the misalignment of the loading beams. Shortening of Columns C12 was taken as the average of the displacements measured by the two cable transducers located at the loading beam. For Column C12-B8, the average displacement was taken as the displacement recorded for Actuator 2, as the displacement transducer for Actuator 1 malfunctioned during testing. Damage of Columns C12 was in the form of bearing failure that involved compressive damage of the concrete, the confining light gauge steel and the internal steel, and separation of the two 6 in x 6 in modules that formed the cross section of the columns (Figure 7). Damage was localized at one end of the columns near the support. The failure initiated with bulging of the light gauge confining steel section and separation of the two 6 in x 6 in sectional modules. At higher loads, the side walls of the light gauge steel buckled, while the confined concrete crushed. Furthermore, the 20M internal bars buckled due to the lack of lateral restraining.

(a) (b) (c) (d)

Figure 7: Damage of Columns C12 at failure: (a) C12-A8; (b) C12-A9; (c) C12-B8; and (d) C12-B9.

3.3 Columns C18 (6 in x 18 in)

Loading of Column C18-B8 was conducted with two actuators, which was slightly modified to conduct the test. Two-1000 kN-capacity actuators were positioned at the ends of the loading beam, and the column was positioned on the opposite side of the loading beam and extended to a reaction frame. This setup with two actuators for Column C18-B8 was not as stable as the subsequent setup with three actuators used for the other C18 columns. As a result, twisting of the loading beam was observed, specifically near the peak load. While the displacement increased in one actuator, it decreased in the other actuator, i.e., Actuator 1 and Actuator 2 moved in opposite directions. Due to the excessive twisting of the loading beam and the lack of actuator capacity to fail the column, the test was halted and then repeated. The first and second tests were named C18-B8-1 and C18-B8-2, respectively. Column C18-B8 showed some damage during the first test, specifically bulging of the light gauge steel and crushing of concrete on the north side near the loading beam, however failure was not experienced until the completion of the second test. Sudden compression failure of the light gauge steel and concrete at the north side of column near the loading beam was observed after sustaining the peak load during the second test (Figure 8(c)). Separation of the three - 6 in x 6 in sectional modules was not observed for Column C18-B8. Loading of the other columns, Columns C18-A8, C18-A9, and C18-B9, was conducted with three actuators, which, in general, was very stable with similar displacement of the actuators up to the peak load. Columns C18-A8, C18-A9, and C18-B9 failed under compression at the ends near the loading beam or the reaction frame. The failure mechanism involved buckling of the light gauge steel and crushing of the concrete along with separation of the three sectional modules (Figure 8).

(a) (b) (c) (d)

Figure 8: Damage of Columns C18 at failure: (a) C18-A8; (b) C18-A9; (c) C18-B8; and (d) C18-B9.

4 Discussion of Experimental Results

The response of the concrete-filled light gauge steel composite columns was assessed against three main design parameters: cross section size, light gauge steel profile, and column length. This assessment is based on the results obtained from the experimental program, which are plotted in Figure 9. Results for Column C18-B8 were not included in Figure 9. Column C18-B8 was tested with two actuators, which did not capture the true peak load capacity of the C18 series of columns. The loading capacity of the two actuators was exceeded, resulting in twisting of the loading system which, in turn, triggered premature localized damage toward one side of the column.

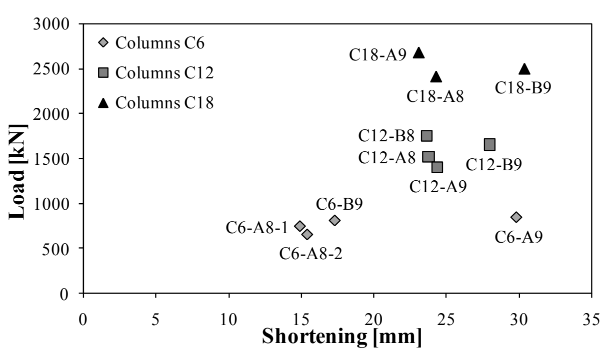

Figure 9: Experimental response of concrete-filled light gauge steel composite columns.

4.1 Cross Section Size

The increase of load capacity was proportional to the cross section size. On average, Columns C12 (6 in x 12 in) and Columns C18 (6 in x 18 in) sustained a load increase of 107% (2.07 times) and 231% (3.31 times) compared with Columns C6 (6 in x 6 in), respectively (Table 4). Average shortening of Columns C12 and C18 were similar and approximately 25 mm, while average shortening of Columns C6 was approximately 16 mm. Due to the non-rigid connection between the sectional modules that were used to construct the C12 and C18 columns, it was expected that the columns would sustain loads proportional to the cross sectional area, but similar shortening. The latter, however, was not realized in part because of the concrete softening effect experienced at the beginning of the loading and end bearing-type failure mode. The peak loads and corresponding shortening averages shown in Table 4 were calculated for the three column cross sections (C6, C12, and C18), except for Column C18-B8 and shortening of Column C6-A9. Column C6-A9 sustained similar load as the other 6 in x 6 in columns, but the shortening was considerably larger, which resulted in a response with approximately half the stiffness of the other three - 6 in x 6 in columns. The location of the connection flaps of the light gauge steel that formed the closed column section along with premature buckling of the steel may have affected the response of Column C6-A9.

Table 4: Effect of cross section on the response of concrete-filled light gauge steel composite columns.

	Cross Section (in x in)	Average Peak Load (kN)	Average Peak Shortening (mm)
C6	6 x 6	763	15.9
C12	6 x 12	1582	25.0
C18	6 x 18	2526	25.9

4.2 Light Gauge Steel Profile

Two light gauge steel profiles, Profile A and Profile B, were used in the construction of the columns. The difference is the type of connection flap that was used to form the light gauge steel section. The average peak load and corresponding shortening were calculated for each light gauge profile (A and B) and for each cross section (C6, C12, and C18) (Table 5). Results for Column C18-B8 and shortening at the peak load for Column C6-A9 were not included due to the deficiencies mentioned above. This permitted a comparison of the effect of the light gauge steel profile for each load level. Due to the limited data from this test program, the results presented in Table 5 do not provide any conclusive trends. Based on the average results, light gauge steel profile B contributed to a load increase of approximately 8% and 17% for Columns C6 and Columns C12, respectively, relative to light gauge steel profile A. For Columns C18, profiles A and B resulted in similar load capacity (difference of approximately 2%). In general, shortening of columns with profile B was slightly larger. Specifically for Columns C18, shortening of the only valid column with profile B was approximately 7 mm larger than the average of two columns with profile A. Shortening values, however, included the effect of concrete softening that varied from section to section.

Table 5: Effect of steel profile on the response of concrete-filled light gauge steel composite columns.

Profile	Columns C6		Columns C12		Columns C18	
	Average Peak Load (kN)	Avg. Peak Shortening (mm)	Average Peak Load (kN)	Avg. Peak Shortening (mm)	Average Peak Load (kN)	Avg. Peak Shortening (mm)
A	748	15.2	1459	24.1	2542	23.7
B	810	17.3	1705	25.9	2495	30.4

4.3 Column Length

The effect of column length is discussed based on the tabulated average peak loads and corresponding column shortenings presented in Table 6, except for the results for Column C18-B8 and the shortening at the peak load for Column C6-A9. In terms of load capacity, there is no definite trend. This is a result of the load capacity being governed by end bearing, which is a sectional limit state and independent of column length. Neither elastic nor plastic buckling of the columns was observed during the tests; therefore, the column length and support condition did not play a significant role in the load capacity. The recorded loads for both lengths are similar and the comparison varies with cross section. For cross sections C6 and C18, the average peak load sustained by 9-ft columns is slightly higher than that sustained by 8-ft columns. For Columns C12, however, 8-ft columns sustained slightly more load than 9-ft columns. Conversely, the shortening values show a trend where the average shortenings measured for the 9 feet-long columns was, in general, approximately 11% higher than the average shortenings measured for the 8 feet-long columns. This increase was in agreement with the expected increase in shortening for elastic response, which is proportional to the ratio of 9-ft to 8-ft (12.5% increase). Due to limited data, additional test results are required to better assess the effect of column length on the response of concrete-filled light gauge steel composite columns.

Table 6: Effect of column length on the response of concrete-filled light gauge steel composite columns.

Length (ft)	Columns C6		Columns C12		Columns C18	
	Average Peak Load (kN)	Avg. Peak Shortening (mm)	Average Peak Load (kN)	Avg. Peak Shortening (mm)	Average Peak Load (kN)	Avg. Peak Shortening (mm)
8	698	15.2	1635	23.8	2408	24.3
9	829	17.3	1528	26.2	2586	26.8

5 Calculated Strength of Columns

From the tests, it was observed that all columns failed by crushing of concrete at one or both ends near the loading beam and/or reaction frame. The internal steel reinforcing bars were well within the elastic range (according to the recorded strains at failure) and were not sufficiently developed in the concrete at the ends of the columns. Furthermore, test results showed that global lateral buckling of the columns was not observed at the peak compressive load capacity. Therefore, the axial strength capacity of the columns, P_n, was assumed to be a combination of the contribution of concrete, C_c, and the contribution of the light gauge steel, F_s.

[1] $$P_n=C_c+F_s$$

The concrete contribution was based on the bearing resistance according to the requirements of the Canadian Standards Association (CSA) Standard A23.3-04 Design of Concrete Structures (clause 10.8.1), and the contribution of the light gauge steel was based on the average strain measured by the strain gauges located at the mid-length of the columns at the peak recorded axial load.

[2] $$C_c=0.85A_c\Phi_c f'_c$$

[3] $$F_s=A_s\Phi_s E_s\varepsilon_s$$

Where A_c is the cross-sectional area of the concrete encased by the light gauge steel, f'_c is the compressive strength of concrete, A_s is the cross-sectional area of the light gauge steel, E_s is the modulus of elasticity of the light gauge steel, ε_s is the average strain of the light gauge steel measured at failure, and Φ_c and Φ_s are the material factors for concrete and steel, respectively, which were set to unity.

The concrete contribution of Columns C6 was calculated using the properties of Column C6-A8, and the concrete contribution of columns C12 and C18 are based on multiples of 2 and 3, respectively, of the C6 bearing strength. The average theoretical bearing capacity of both profiles A and B are compared with the corresponding average experimental results in Table 7. Note that the average stress in the light gauge steel corresponding to the peak axial load capacity of the column was approximately 148 MPa.

Table 7: Experimental and theoretical bearing capacity of concrete-filled light gauge composite columns.

Column	Cross Section (in x in)	Calculated Load (Cal) Concrete (kN(%))	Calculated Load (Cal) Steel (kN(%))	Calculated Load (Cal) Total (kN)	Experimental Load (Exp) Total (kN)	Cal/Exp
C6-A8-1	6 x 6	628(87%)	94(13%)	722	745	0.97
C6-A8-2	6 x 6	628(92%)	57(8%)	685	651	1.05
C6-A9	6 x 6	628(83%)	128(17%)	756	847	0.89
C6-B9	6 x 6	628(84%)	116(16%)	744	810	0.92
C12-A8	6 x 12	1256(88%)	176(12%)	1432	1517	0.94
C12-A9	6 x 12	1256(88%)	168(12%)	1424	1400	1.02
C12-B8	6 x 12	1256(84%)	244(16%)	1500	1753	0.86
C12-B9	6 x 12	1256(89%)	148(11%)	1404	1656	0.85
C18-A8	6 x 18	1884(85%)	320(15%)	2204	2408	0.92
C18-B9	6 x 18	1884(86%)	299(14%)	2183	2495	0.87
Average						**0.93**
COV						**7.26 %**

6 Conclusions

The compressive strength capacity of twelve concrete-filled light gauge steel composite columns was experimentally determined in this study. Three parameters were investigated: cross section size (6 in x 6 in, 6 in x 12 in, and 6 in x 18), column length (8 ft and 9 ft), and cross section profile (A and B). In addition, the axial compression strength capacity of the columns was predicted according to CSA Standard A23.3-04.

The load capacity of the composite columns was proportional to the cross section. Columns C12 (6 in x 12 in) and Columns C18 (6 in x 18 in) sustained approximately double and triple the load of Columns C6 (6 in x 6 in). Compression shortening of Columns C6 was slightly lower than that of columns C12 and C18. Compression softening at the ends of the columns affected the shortening of the columns, which were expected to be similar based on the proportional axial stiffness of the columns.

Columns with light gauge steel profile B sustained higher load and larger shortening than those with light gauge steel profile A, specifically Columns C6 and C12. The light gauge steel profiles A and B had similar effect on the compressive strength of Columns C18. Shortening, however, was slightly greater for profile B. These observations are not conclusive due to the limited number of tests conducted.

The column compressive capacities were controlled by end bearing, which is a cross sectional limit state independent of length and support condition. The measured shortening of the columns were proportional to the length, which indicates both column lengths sustained similar shortening strains.

The capacity of the concrete-filled light gauge steel columns was estimated with end bearing resistance as the limit state according to CSA A23.3-04. This calculation did not include any contribution from the internal steel reinforcing bars. The calculated to measured axial strength capacity was 0.93.

7 References

ASTM International. 2009. Standard Test Method and Definitions for Mechanical Testing of Steel Products. ASTM A370-09. West Conshohocken, PA, USA: 47p.

ASTM International. 2009. Standard Test Method for Compression Strength of Cylindrical Concrete Specimens. ASTM C39/C39M-09a. West Conshohocken, PA, USA: 7p.

Canadian Standards Association (CSA). 2004. Design of Concrete Structures. CAN/CSA-A23.3-04. Mississauga, ON, Canada: 214p.